

“GRAPH CUT BASED IMAGE SEGMENTATION USING STATISTICAL PRIORS AND ITS  
APPLICATION TO OBJECT DETECTION AND THIGH CT TISSUE  
IDENTIFICATION ANALYSIS”

by

TAPOSH BISWAS

A THESIS

Submitted in partial fulfillment of the requirements  
for the degree of Master of Science in the  
Natural Resources Graduate Program  
of Delaware State University

DOVER, DELAWARE

May 2018

This thesis is approved by the following members of the Final Oral Review Committee:

Dr. Sokratis Makrogiannis, Committee Chairperson, Department of Mathematical Science,  
Delaware State University

Dr. Thomas A. Planchon, Committee Member, Department of Physics and Engineering, Delaware  
State University

Dr. Qi Lu, Committee Member, Department of Physics and Engineering, Delaware State  
University

Dr. Matthew Tanzy, External Committee Member, Department of Mathematical Science,  
Delaware State University

**COPYRIGHT**

Copyright ©2018 by Taposh Biswas. All rights reserved.

## DEDICATION

This thesis is dedicated to my parents Monoranjan Biswas and Dipti Biswas who have supported curiosity throughout my life. Without their persistent guidance, support, and advice, the successes I have achieved till now would never have come to fruition.

## ACKNOWLEDGEMENTS

First, I would like to thank Dr. Sokratis Makrogiannis for giving me the opportunity to be a part of his research group (MIVIC) and supporting me through my thesis. It is an honor to work with him; he was always there for helping me improve my programming skills and assisting me with my research. I really appreciate his contributions of time, ideas and funding to complete my master's degree. His door was always to discuss about any problem. I would like to thank the Federal Research and Development Matching Grant Program of the Delaware Economic Development Office (DEDO) for the funding and giving me the opportunity to complete my degree. Thanks to my research group (MIVIC) for encouraging me, working with me and assisting me. I would like to thank my committee members Dr. Lu, Dr. Planchon, Dr. Tanzy for their time, interest, and insightful comments regarding my dissertation. I would like to thank my mom (Dipti Biswas) my dad (Monoranjan Biswas), family and friends for always supporting me and constantly encouraging me to do better. I would like to thank my Sister Anju Biswas to stand by my side always.

## ABSTRACT

Image segmentation is a field of image analysis that aims to partition an image scene into regions corresponding to objects. It is a popular research topic of image analysis with many applications to the computer vision and medical imaging domains including object recognition and delineation of anatomical structures and tissues. The goal of this thesis is to investigate whether graph cut techniques can be used to delineate the objects in a visual scene for biomedical and computer vision applications. The graph cuts method is one of the leading automated segmentation methods for 2D and 3D images. It delineates the regions by creating graph partitions and finds the optimal graph partition by minimizing an energy function that consists of data and smoothness terms. Graph cuts represent the set of pixels in the image using graph vertices. Relationships between pixels are represented by graph edges and expressed by the smoothness term of the energy function. Source and sink nodes are introduced to the graph to model the region prior information that is used in the data term. An advantage of this method is that it can combine local and global visual information to obtain segmentation of the objects in the visual scene. We perform image segmentation on a database of generic images with reference region masks to illustrate and evaluate the applicability of this method. We applied this technique to generic and medical imaging data for tissue identification. To accomplish that we used two methods one is GC (graph cut) with k means and GC with prior knowledge. We obtained more accurate segmentation results using GC with prior probability (supervised reference masks or polylines) than GC with k-means (automated image segmentation).

## TABLE OF CONTENTS

LIST OF FIGURES .....	vii
LIST OF TABLES .....	viii
CHAPTER I: INTRODUCTION.....	1
1.1 Image Segmentation.....	1
1.2 Significance of Image Segmentation.....	2
1.3 Hypothesis.....	2
CHAPTER II: PRINCIPLES OF GRAPH CUT OPTIMIZATION.....	7
2.1 Introduction to Flow Networks or Graphs .....	7
2.3 Maximal Flows and Minimal Cuts on Graphs .....	11
2.3.1 Min-Cut-Max-Flow Theorem.....	12
2.4 Min Cut Algorithm.....	16
2.5 Calculation of Maximal Flow .....	18
2.6 Augmented Path .....	18
2.7 Push-relabel Algorithm .....	18
2.8 Boykov and Kolmogorov New Algorithm.....	19
2.9 Application of Graph Cuts .....	21
2.10 Energy minimization using graph cut .....	23
CHAPTER III: GRAPH CUT SEGMENTATION WITH STATISTICAL PRIORS.....	26
3.1 Learning Parametric Models for Tissues .....	26
3.2 Unsupervised Learning: K-means clustering:.....	26
3.3 Segmentation using Supervised Learning for Prior Statistics.....	27
3.4 Object Detection and Recognition .....	29
3.5 Automated Medical Image Segmentation Techniques.....	30
3.6 Computed Tomography Imaging. ....	31
3.7 Calculation of Priors for Segmentation of Medical Images.....	32
CHAPTER IV: EXPERIMENTS, COMPARISONS AND RESULTS.....	33
4.1 Experiment 1: Object detection.....	33
4.2 Experiment 2: Thigh CT tissue identification.....	36

CHAPTER V: CONCLUSION AND FUTURE WORK .....	40
5.1 Conclusion.....	40
References.....	41

## LIST OF FIGURES

Figure 1 : Undirected example graph [20]. Edges are labelled. Terminal nodes are box-shaped. .	9
Figure 2 : Example graph $G = \{u, v\}, \{e\}$ consisting of two nodes $u, v$ and one edge $e$ [20]. $e$ has (undirected) capacity 10 and the flow on it is $f_{u,v} = 3$ . Left: Flow network. The diamond shaped arrowhead of the edge indicates flow direction. Right: Corresponding residual flow network. In the residual network, the edge from $u$ to $v$ has residual capacity $10-3 = 7$ , and $c_{v,u} = 10-3 = 13$ .	10
Figure 3: Example of undirected graph transporting a flow [20]. The diamond shaped edge endings indicate the direction of the flow. Note that the flow is not a maximum flow, since e.g. the path $s \rightarrow v_1 \rightarrow v_3 \rightarrow t$ could still be augmented.	12
Figure 4: Original network of max flow.	16
Figure 5: Min-cut of the graph.	17
Figure 6: Flowchart of the Graph Cut method.	22
Figure 7: Energy minimization via graph cuts.[22]	23
Figure 8: Segmentation results on two test images from our database. First column: original images, second column: reference images, third column: Auto (k-clustering) method, Fourth column: using object prior.	34
Figure 9: Graph corresponds to the two methods of Table 1,	35
Figure 10: Tissue identification results on two test images from our Thigh BLSA CT images database. First column: original images, second column: reference images, third Column: GC with ROI prior, Fourth column: GC with K means prior.	37



## LIST OF TABLES

Table 1: Mean and Standard Deviation of two different graph cut techniques. ....	34
Table 2: Result after using manual method – GC with object priors.....	35
Table 3: Results of Auto method- conventional graph cuts.....	36
Table 4: Mean and standard deviation of DSC for two graph cut techniques for each tissue of thigh CT .....	38

## CHAPTER I: INTRODUCTION

### 1.1 Image Segmentation

Image segmentation is the process of partitioning a digital image into multiple regions using pixels or voxels. It is used to identify objects or other relevant information of an image into something that is more meaningful to analyze the image. There are many ways to perform image segmentation. Here we study graph cut techniques for image segmentation.

The graph cuts method is powerful for image segmentation. In the last few years these methods have become very popular. Graph cuts are applicable to many computer vision applications. There are many publications about segmentation methods using graph cuts [1,2]. The estimation of optical flow problems and stereo vision problems are frequently treated by graph cuts. There are several widely used graph cut based algorithms for scene reconstruction from multiple views. Graph cut methods are not only limited to image processing and computer vision, but they are also well-suited for minimizing discrete functions and could be applied to several optimization problems with certain properties. As an example in the machine learning research area, graph cut ideas are used in semi-supervised learning, where one tries to expand the small set of labeled data with these methods. Another field where graph theoretic methods play an important role is spectral clustering. Here one tries to cluster a graph whose vertices represent data measurement points and edges represent the similarity of these data points. [3, 4, 4]. The interesting part of spectral clustering methods is that they try to solve the problems by analyzing eigenvalues and eigenvectors of matrices that can be computed from the graphs.

In all graph cut optimization methods, the procedures fundamentally the same. We formulate an appropriate discrete cost function for the given problem. Then a structure consisting of nodes and

arcs is constructed to represent the graph. Then this graph will be divided or cut into two subgraphs. We can identify a solution of cost function by this partition of graph. Then after finding a minimal cut, we search for a solution of objective function with minimal energy.

## **1.2 Significance of Image Segmentation**

Image segmentation is useful for analyzing the content of an image. Image segmentation tools are used for medical image processing analysis and other applications. It may be use for analyzing brain MRI data and anatomical structures; detecting multiple sclerosis, tissue structures, cells, muscle blood vessels, quantification, surgical planning and many more tasks. In oncology applications, image segmentation is used to locate tumors and other pathologies. Other applications of image segmentation are machine vision, face recognition, fingerprint recognition, stereo vision, traffic control systems, locating objects in satellite imagery, etc. Graph cut techniques are also useful in every day applications such as image cropping, n-dimensional image segmentation, colorization, image reconstruction, image editing and more.

## **1.3 Hypothesis**

There are numerous methods for performing image segmentation [6]. Here we are using the graph cuts method to segment images. The graph cuts method is very effective for object detection and segmentation of generic and biomedical images.

We hypothesize that the use of more accurate statistical priors will improve the segmentation accuracy of graph cuts compared to generic terminal node prototyping techniques such as k-Means [7]. So, we study and propose techniques for building and introducing priors into the graph cut optimization method.

Graph cuts are very popular techniques and applicable to many computer vision tasks. There are many publications about segmentation methods using graph cuts. The estimation of optical flow problems and stereo vision problems are frequently treated by graph cuts. There are several prosperous graph cut based algorithms for scene reconstruction from multiple views. Graph cut methods are not only limited to image processing and computer vision, but they are also well-suited methods for minimizing discrete functions and could be applied to several problems with specified conditions. As an example in the machine learning research area, graph cut techniques are used for data clustering.

## **1.4 Survey of Literature**

### **Edge Based Image Segmentation**

Edge based segmentation identifies edge pixels and links them together to form contours [8]. Edge detecting operators are used to locate the edges of an image. With the help of spectral methods and the morphological algorithm of watershed, Fernando C. Monteiro [9] proposed a new image segmentation method of edge and region based information. Primarily, they use bilateral filtering to reduce the noise from image, next, they use region merging to perform preliminary segmentation, generate region similarity and then they perform graph-based region grouping using Multi-class Normalized Cut method [10]. Weihong Cui Yi Zhang [11] proposed an edge based image segmentation to generate multi-scale image segmentation. They use band weight and NDVI (Normalized Difference Vegetation Index) to calculate edge weight. Edge based threshold method to perform image segmentation. They perform experiments on multi-scale resolution images, i.e., Quick-bird multispectral images. This method maintains the object information and keeps object

boundaries while segmenting the images. Using variance filter Anna Fabijańska [12] proposed a new method for edge detection in image segmentation process.

### **Region-Based Image Segmentation**

A region  $R$  of an image  $f$  is defined as a connected homogenous subset of the image with respect to some criterion such as gray level or texture [12]. A segmented image  $f$  is a partition of  $f$  into several homogeneous regions  $R_i, i = 1, \dots, m$ . An image  $f$  can be segmented into regions  $R_i$  such that:

1.  $f = \cup_{i=1}^m R_i$
2.  $R_i \cap R_j = \emptyset, 1 \leq i, j \leq m \wedge i \neq j$
3.  $P(R_i) = \text{true for all } i$
4.  $P(R_i \cup R_j) = \text{false}, 1 \leq i, j \leq m \wedge i \neq j$  and  $R_i$  and  $R_j$  are adjacent

Region based segmentation considers gray-levels from neighboring pixels using one of the three basic approaches, region merging, region splitting, and split-and-merge region growing [13].

Region based methods are robust because regions cover more pixels and there are ways to have more information available in order to characterize region –for example using texture it is possible to detect a region which is not easy when dealing with edges region growing techniques are generally more effective on noisy images, where edges are difficult to detect.

### **Thresholding:**

Objects can be easily separated from the background using thresholding techniques when grey levels of pixels of objects are quite different from those of background [14]. These techniques are also used in applications such as, “Document image analysis, Map processing, Scene processing, Inspection of materials for quality, Cell imaging, Knowledge representation, Non-destructive testing, Ultrasonic, eddy current and thermal images, X-ray computed tomography and Endoscopic images etc” besides image segmentation [14]. Thresholding converts the gray scale image into a binary image where “one state will indicate the foreground objects, other state will correspond to the background. Depending on the application, the foreground can be represented by gray-level 0, that is, black as for text, and the background by the highest luminance for document paper that is 255 in 8-bit images, or conversely the foreground by white and the background by black” [14]. Authors of [14] have placed the thresholding techniques in to following six categories: Histogram shape-based methods, Clustering-based methods, Entropy-based methods, Object attribute-based methods, Spatial methods and Local methods. Orlando J Tobias et al [15] have proposed “an approach for histogram thresholding according to the similarity between gray levels” because “methods for histogram thresholding based on the minimization of a threshold-dependent criterion function might not work well for images having multimodal histograms”. To overcome the local minima, authors have used a fuzzy measure for assessing the similarity between grey levels.

### **Clustering:**

Mac Queen [16] introduced K- Means that is one of the most popular partition-based clustering algorithms in the year of 1967 to solve various clustering problems. This algorithm aimed to group data into k clusters built on randomly selected initial centroids. The grouping is organized by minimizing the Euclidean distances between the data points and their associated centroid

[17]. Clustering is a partition of images or data into different categories of related objects. Each individual group called cluster contains objects, which are related between them, and variant differentiate to the objects of further group [17]. K-means is well known partitioning method that uses an iterative approach. The k-means algorithm has the following important properties: (1) It may be applied for large dataset processing. (2) It often terminates at a local optimum. (3) The clusters have convex shapes [18] (4) It works only on numeric values.

### **Graph-based segmentation:**

Nowadays graph-based segmentation is a popular area in research [19]. Graph-based image segmentation techniques in most case represent the problem in terms of a graph  $G = (V, E)$  where each node  $v_i \in V$  corresponds to a pixel in the image, and edges  $(v_i, v_j) \in E$  corresponding to pairs of neighboring vertices. Each edge  $(v_i, v_j) \in E$  has a corresponding weight  $w((v_i, v_j))$ , that is a non-negative measure of the dissimilarity between neighboring elements  $v_i$  and  $v_j$  [55]. In image segmentation, the weight of an edge is some measure of the dissimilarity between the two pixels connected by that edge and the elements in  $V$  are pixels. In the graph-based approach, a segmentation  $S$  is a partition of  $V$  into components such that each component (or region)  $C \in S$  corresponds to a connected component in a graph  $G' = (V, E')$ , where  $E' \subseteq E$ . Particularly, any segmentation is induced by a subset of the edges in  $E$ . There are many ways to measure the quality of a segmentation but usually we want the elements in a component to be similar, and elements in different components to be dissimilar. It implies that edges between two vertices in the same component should have low weights, and edges between vertices in different components should have higher weights.

## CHAPTER II: PRINCIPLES OF GRAPH CUT OPTIMIZATION

Here we will describe basic theoretical concepts in order to be able to apply graph cuts on real imagery later on. First, we will define basic terminology and concepts of graph theory and flow networks. Then we will prove the result that is very important to graph partitioning, min-cut-max-flow theorem, and describe optimization algorithms.

### 2.1 Introduction to Flow Networks or Graphs

Here, we will define and describe what we will call a graph throughout this document [20]. Before definitions, we should remark that graph is also known under the name flow network in the majority of the graph theoretical literature. In this document, we will use both ideas.

A flow network or graph,  $G = \{V, E\}$  consists of nodes and edges where the set of nodes  $v \in V$  and the set of edges  $e \in E$ .

- We will work with undirected graphs for our applications.
- We will now define properties and invariants of graphs, but before that, we should get an idea about flow network.

An example (among many others) is the sewage water system of a city:

- It consists of a large network of water pipes. These pipes often join, or one pipe ends in another pipe.
- All these junctions match with graph nodes, the reason is only there two or more pipes can be connected.
- Now, we will define two important functions on graphs: the capacity and the flow between two adjacent nodes.



- For the sewage system example, we need to identify the diameter of a pipe with the capacity of the corresponding edge. If the diameter of the pipe is large, more water can flow through it.

The pipe will take the water from one to another place. Connected houses and drain are source and the river could be the sink. The pipe cannot carry more water than its capacity otherwise, pipe will burst.

The capacity is a function

$$c: E \rightarrow R_0 +$$

Sometimes it indicates each edge as a non-negative value, the weight of an edge is known as its capacity. To emphasize the direction of flows and capacities, here we will use a different version of the capacity function by the two nodes and they are connected by this edge:

$$c: V \times V \rightarrow R_0 +$$

We can also define the capacity of a directed edge. The flow is a function

$$f: V \times V \rightarrow R$$

This is a real value of each edge. In figure 1, an example of a flow network can be seen. It is important to note that the flow and the capacity functions are defined as quantities of one edge. If there is no edge between two nodes, then the flow and capacity between them is zero. For example, flow and capacity between node  $s$  and  $v_3$  in figure 1 are zero.

A property of a flow function is its skew symmetry, and it is expressed by

$$f(u, v) = -f(v, u) \quad (1)$$

This rule implies that if there are more than one edges on the path between two nodes  $u$  and  $v$ , the flow function resembles the accumulated flow over all these edges. A single edge connects two single nodes only.

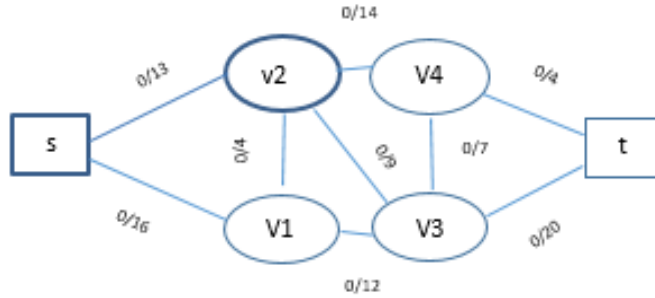


Figure 1 : Undirected example graph [20]. Edges are labelled. Terminal nodes are box-shaped.

For two subsets of the node set  $X, Y \subset V$ , we can define the net flow from  $X$  to  $Y$  as

$$f(x, y) := \sum_{u \in X} \sum_{v \in Y} f(u, v) \quad (2)$$

The **Kirchhoff's law** (At any node (junction) in an electrical circuit, the sum of currents flowing into that node is equal to the sum of currents flowing out of that node or equivalently) can then be expressed as

$$\sum_{v \in V} f(u, v) = 0, \forall u \in V \quad (3)$$

Where  $T \subset V$  is the set of all terminal nodes. In our applications, we will have two terminal nodes, one source node and one sink node. The source node is denoted by  $s$  and the sink node is denoted by  $t$ . The following condition must be satisfied for each edge:

$$f(u, v) \leq c(u, v), \forall u, v \in V \quad (4)$$

Another important quantity for flow networks is the so-called residual capacity. **Residual capacity** expresses how much water the pipe can transport.

It is defined as a function  $c_f$ :

$$c_f: V \times V \rightarrow \mathbb{R}_0^+$$

This function returns the amount of flow, that, given a flow  $f$ , an edge still could carry, and can be computed by

$$c_f(u, v) = c(u, v) - f(u, v) \tag{5}$$



Figure 2 : Example graph  $G = \{u, v\}, \{e\}$  consisting of two nodes  $u, v$  and one edge  $e$  [20].  $e$  has (undirected) capacity 10 and the flow on it is  $f(u, v) = 3$ . Left: Flow network. The diamond shaped arrowhead of the edge indicates flow direction. Right: Corresponding residual flow network. In the residual network, the edge from  $u$  to  $v$  has residual capacity  $10 - 3 = 7$ , and  $c_f(v, u) = 10 - (-3) = 13$ .

Then the residual network of an undirected graph is a directed graph, because if an edge has a current flow, then the residual capacity in the direction of the flow is smaller than in the opposite direction. This effect is illustrated in figure 2 with one edge between two nodes. Let a directed edge from  $u$  to  $v$  have capacity  $C$ . If no flow is on that edge, we have  $c(u, v) = C$  and in the opposite direction  $c(v, u) = 0$ . Also for the residual capacities, we get  $c_f(u, v) = C$  and  $c_f(v, u) = 0$ . Now suppose there is a flow  $F \leq C$  on that edge from  $u$  to  $v$ . The residual capacity in direction of the flow changes as expected:  $c_f(u, v) = C - F \geq 0$ . The opposite direction residual capacity which was zero before, now is

$$c_f(v, u) = c(v, u) - f(v, u) = 0 - (-F) = F \quad (6)$$

This means by sending a flow along  $(u, v)$ , a new edge has been added to the residual network.

### 2.3 Maximal Flows and Minimal Cuts on Graphs

In this thesis we study graphs as well as cuts of such graphs. Let's assume that  $G = \langle V, E \rangle$  has two terminal nodes, a source  $s$  and a sink  $t$ ,  $\{s, t\} = T \subset V$ .

A cut  $C \subset E$  on a graph  $G$  is a subset of the edge set having the property that in the induced graph

$$G^C := \langle V, E \setminus C \rangle$$

The terminal nodes are separated from each other and the set of nodes  $V$  is partitioned into two sets  $V_s$  and  $V_t = V - V_s$ . Each of the parts has exactly one terminal node as element, i.e.  $s \in V_s$  and  $t \in V_t$ . Cut will not contain more edges than necessary. Cuts will not have a proper subset that would still separate the terminals. Otherwise, the edge set of a graph itself would be a cut, which does not make sense. These are restrictions for our considerations on cuts in this section to the case of a separating two terminal nodes only. Given this formulation, now we can define the capacity and the flow of a cut. The capacity of a cut is the sum of the capacities of all its edges. Here we define cut as  $c(C)$

$$c(C) = \sum_{e \in C} c(e) = \sum_{u \in V_s} \sum_{v \in V_t} c(u, v) \quad (7)$$

Similarly, the flow of a cut is defined as the sum of the flow on the edges of cut  $C$

$$f(c) = \sum_{(e \in C)} f(e) = f(v_s, v_t) \quad (8)$$

The edges cross the cut and that is for an (undirected) edge  $e$  from  $u$  to  $v$  that either  $u \in V_s$  and  $v \in V_t$ , or  $u \in V_t$  and  $v \in V_s$ . Cuts are defined in a different way in directed graphs. An edge is a part

of the cut when it is directed from  $V_s$  to  $V_t$ . Then, the capacity and flow of that edge can be calculated as for undirected graphs. The flow of a graph is defined as the sum of flow leaving the source or the sum of flow entering the sink of the graph.

$$|f(G)| = \sum_{u \in v} f(s, u) = \sum_{u \in v} f(u, t) \quad (9)$$

As in the sewage system of a city there will be certain maximal amount of water and will be transported, so every flow network has a uniquely determinable maximal flow value. If a graph is at maximal flow it's not possible to increase the flow, because there doesn't exist path with residual capacity that could be augmented.

### 2.3.1 Min-Cut-Max-Flow Theorem

Before the Min-Cut-Max-Flow theorem itself, we need to state and prove a few corollaries in order to prove the theorem.

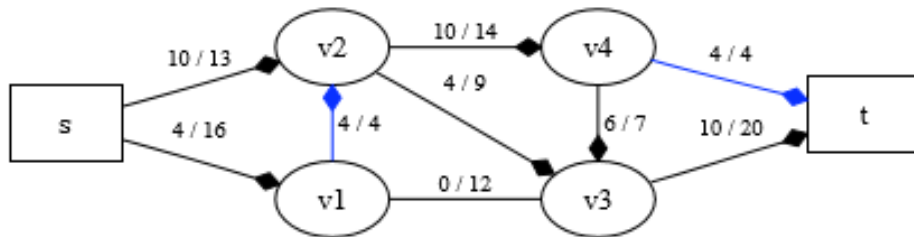


Figure 3: Example of undirected graph transporting a flow [20]. The diamond shaped edge endings indicate the direction of the flow. Note that the flow is not a maximum flow, since e.g. the path  $s \rightarrow v1 \rightarrow v3 \rightarrow t$  could still be augmented.

Here, we assume a graph  $G = \langle V, E \rangle$  with two terminals  $\{s, t\} = T \subset V$ . Let  $C \subset E$  be a cut partitioning the node set  $V = V_s \cup V_t, V_s \cap V_t = \emptyset$ . So that we can state the following corollaries:

### Corollary 1

For a flow  $f$  on  $G$ , the following properties hold true:

1. for any  $X \subset V$  holds:  $f(X, X) = 0$
2. for all  $X, Y \subset V$  we have  $f(X, Y) = -f(Y, X)$
3. For all  $X, Y, Z \subset V$  with  $X \cap Y = \emptyset$  it holds that  $f(Z, X \cup Y) = f(Z, X) + f(Z, Y)$

### **Proof**

From equation (1) we get

$$1. \quad f(x, y) := \sum_{u \in x} \sum_{v \in y} f(u, v)$$

For this summation, each pair of elements of  $X$  appears twice, as  $(u, v)$  and as  $(v, u)$ . With the skew symmetry (1), we can prove that the elements of the summation cancel out in pairs.

2. With equations (2) and (1) we can show

$$\begin{aligned} f(x, y) &:= \sum_{u \in x} \sum_{v \in y} f(u, v) \text{ From (1)} \\ &:= \sum_{u \in x} \sum_{v \in y} -f(v, u) \text{ From (2)} \\ &:= -\sum_{u \in x} \sum_{v \in y} f(v, u) := -\sum_{v \in y} \sum_{u \in x} f(v, u) = -f(y, x) \end{aligned}$$

3.  $f(Z, X \cup Y) = \sum_{u \in z} \sum_{v \in x \cup y} f(u, v) = \sum_{u \in z} \sum_{v \in x} f(u, v) + \sum_{u \in z} \sum_{v \in y} f(u, v)$   
 $f(Z, X) + f(Z, Y)$

### Corollary 2

The flow of a cut and the flow of the graph are equal.

$$F(v_s, v_t) = |f(g)| \tag{10}$$

Proof: From corollary 1-

$$f(V_s, V) = f(V_s, V_s \cup V_t) = f(V_s, V_s) + f(V_s, V_t)$$

Now the flow of the cut is

$$\begin{aligned} f(V_s, V_t) &= f(V_s, V) - f(V_s, V_s) \\ &= f(V_s, V) \\ &= f(s \cup (V_s \setminus s), V) \\ &= f(s, V) + f(V_s \setminus s, V) \\ &= f(s, V) \\ &= |f(G)| \end{aligned}$$

### Corollary 3

The capacity of any cut of that graph will be larger than the value of a flow in a graph.

Proof: we have

$$\begin{aligned} |f(G)| &= f(V_s, V_t) \\ &= \sum_{u \in v_s} \sum_{u \in v_t} f(u, v) \\ &\leq \sum_{u \in v_s} \sum_{u \in v_t} c(u, v) \end{aligned}$$

$$=c(V_s, V_t)$$

### Min Cut Max flow Theorem Proof [20]

Let  $G = V, E$  be a graph, and let  $s, t \in V$  be the two terminal nodes. The value of the max flow is equal to the value of the min cut. There are three equivalent statements

1.  $f$  is a maximal flow
2. There is no augmenting path in the residual graph  $G_f$ .
3.  $f(G) = c(C)$  For some cut  $C$ .

(3)  $\Rightarrow$  (1) by corollary 3, we have that any cut can at most be equal to the capacity of any flow on  $G$ .

$$|f(G)| \leq c(V_s, V_t)$$

From (3) it follows that

$$|f(G)| = c(V_s, V_t)$$

In this matter  $f(G)$  cannot be larger and is a maximum flow



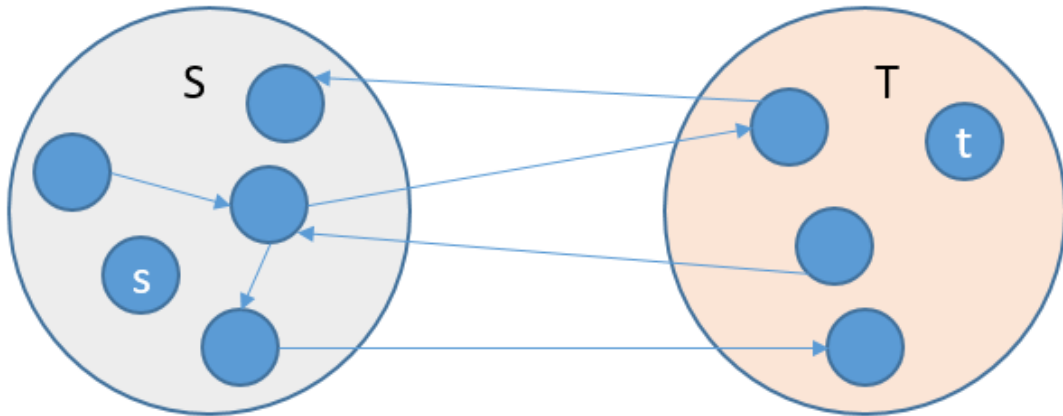


Figure 4: Original network of max flow.

## 2.4 Min Cut Algorithm

Let  $G = (V, E)$  be a connected and undirected multigraph that has  $n$  vertices. A multigraph contains multiple edges between any pair of vertices. A cut in graph  $G$  is a set of edges. A min cut is a cut of minimum cardinality. The graph represents a network and now we can quantify how robust it is in the sense of the minimum number of the links and if it fails network will be disconnected. The min cut algorithm aims to find a cut in minimum size.

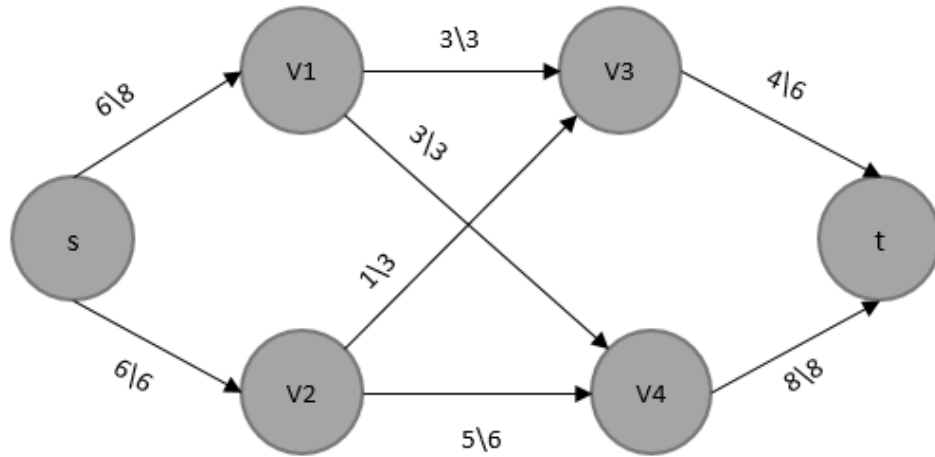


Figure 5: Min-cut of the graph.

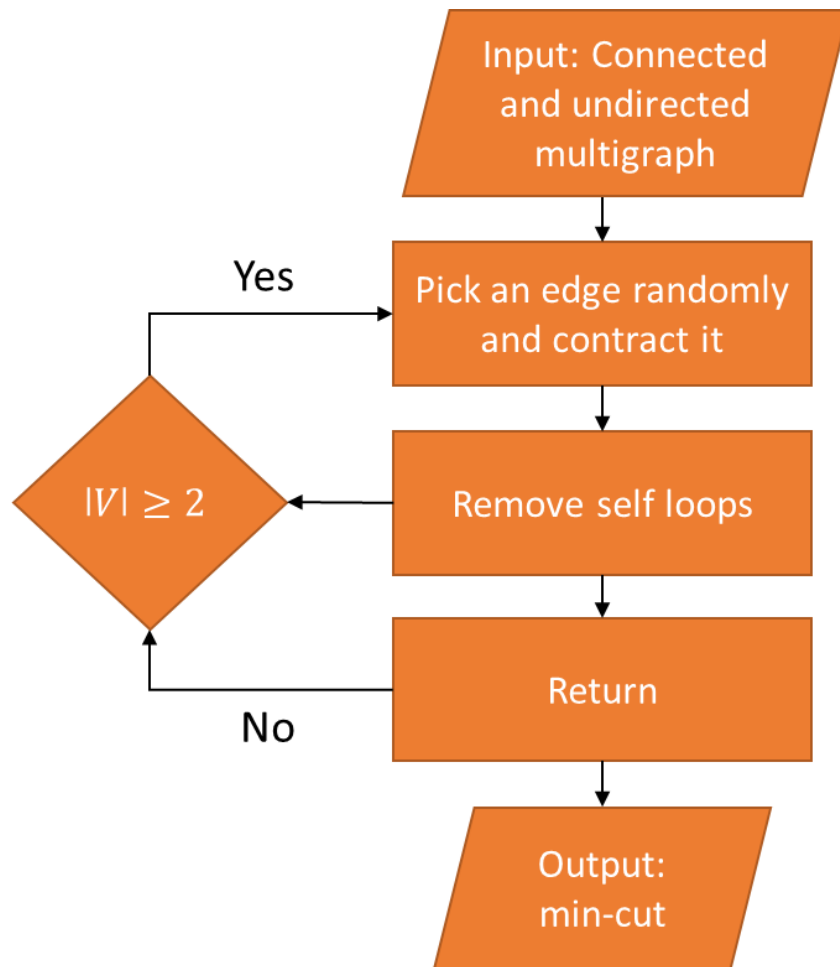


Figure 6: Flowchart of the min-cut algorithm.

## 2.5 Calculation of Maximal Flow

It turns out that computation of the maximal flow is the most costly part of the whole algorithm in terms of computational load. Minimal cut determination is not more expensive than the maximal flow is. The exploration of the connected graph should not cost more than  $O(|V|)$  operations, and the following decision for each edge, whether it is a cut edge or not is one iteration over all edges,  $O(|E|)$ . Here we describe the Augmented Path algorithm. A competing class of algorithms are so-called push-relabel algorithms that we discuss after the augmented path technique.

## 2.6 Augmented Path

To get the maximum flow in the graph augmented paths algorithm work by pushing flow along non-saturated paths from the source to the sink. Augmented path algorithms continuously documents information about the distribution of the current s/t flow denoted  $f$  among the edges  $G$  using a residual graph  $G_f$ . Firstly, there is no flow from the source to the sink. With each new iteration, the algorithm finds the shortest s/t path along the non-saturated edges of the residual graph. After finding the path, the flow is implemented by pushing the maximum possible flow that saturates at least one of the edges in the path. Each augment increases the total flow from the source to the sink  $f = f + df$ . Then a new s-t path is found and then keep repeating the previous steps until no new path is found. When any s/t path crosses, at least one saturated edge in the residual graph then the maximum flow is found. Finally, the s and t graph nodes are separated. For improving theoretical running time complexities for algorithms based on augmenting paths the use of the shortest path is very important.

## 2.7 Push-relabel Algorithm

A labeling of nodes with a lower bound estimate of its distance to sink node along the shortest one saturated path is maintained by push-relabel algorithm for maximum flow optimization.

1. Initially we need to push as much flow as possible to all nodes connected to the source.
2. Pick a node  $u$  with excess flow
3. Pick an edge  $(u, v)$  with an excess capacity where  $v$  has a label that is one less than  $u$ .
4. Push as much flow as possible to  $v$
5. If not possible increase the label of  $u$
6. Rinse and repeat 1
7. Think of label as the distance from the sink.

## **2.8 Boykov and Kolmogorov New Algorithm**

To improve empirical performance of standard augmented path techniques on graphs in vision Boykov, Kolmogorov developed a new algorithm. The new algorithm developed is based on augmented paths by building search trees for detecting augmented paths in Figure 6.

- Two non-overlapping search trees are built one from the source and one from the sink.
- In tree  $S$ , all edges from each parent node to its children are non-saturated.
- In tree  $T$ , edges from children to their parents are non-saturated.
- Nodes that do not belong to  $S$  or  $T$  are called free nodes.
- Nodes in a search tree can be either active or passive.

- The tree is grown until the sink is part of the tree.

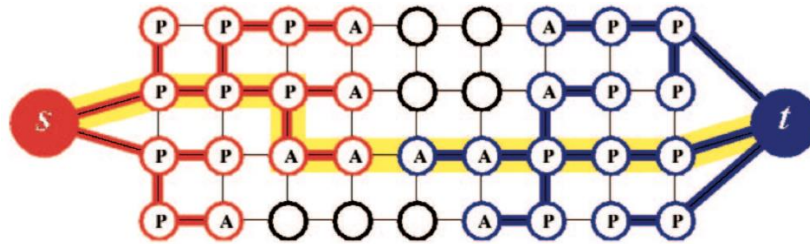


Figure 7: Search trees S and T at the end of growth step. []

### 1. Growth stage

The tree is grown until the sink is part of the tree

- The search tree S and T are expanded
- Active nodes explore adjacent non-saturated edges and acquire new children from a set of free nodes.
- New nodes become active members of the corresponding search tree.
- An active node becomes passive when all neighbors of a given active node are explored.
- The growth stage terminates when an active node encounters a neighboring node that belongs to the opposite tree.

### 2. Augmentation

The found path is augmented and search tree breaks into forest

- Augment the path found at the growth stage
- Some edges in the path become saturated because of pushing through the largest flow possible

- Some of the nodes in the tree S and T may become orphans. The edges linking them to their parents are no longer valid.
- The augmented phase may split the search tree S and T into forests.
- The source s and the sink t are still roots of two of the trees, while orphans from roots of all other trees

### **Adaption**

The S and T trees might be split into forests after the augmentation step. The orphan nodes, that act as roots for trees in the formed forests will either be adopted to the S or T trees or declared free nodes in the adoption step. In this step, a new valid parent is searched for each orphan node. The parent has to belong to the same tree as the orphan and should be connected to this through a non-saturated edge. The node is removed from the tree it belongs to (S or T) If no parent is found for the orphan node, being declared a free node. In this case, all its former children are also labeled as orphan nodes and need to be submitted to the adoption process. The adoption step terminates when all orphan nodes have been either adopted or labeled as free. The role of this step is to restore the structure of the S and T trees to singletree with roots in nodes s and t.

### **2.9 Application of Graph Cuts**

In this thesis, the main concept is the application of the graph cut method for segmentation. First, we create a graph based on the original images using graph cut techniques. Then by using prior information, we can detect the object and background. Cost of edges for s and t link are compared for the whole image. We can get max flow by using max-flow graph optimization. Finally, s-t cut defines a segmentation of the original image.

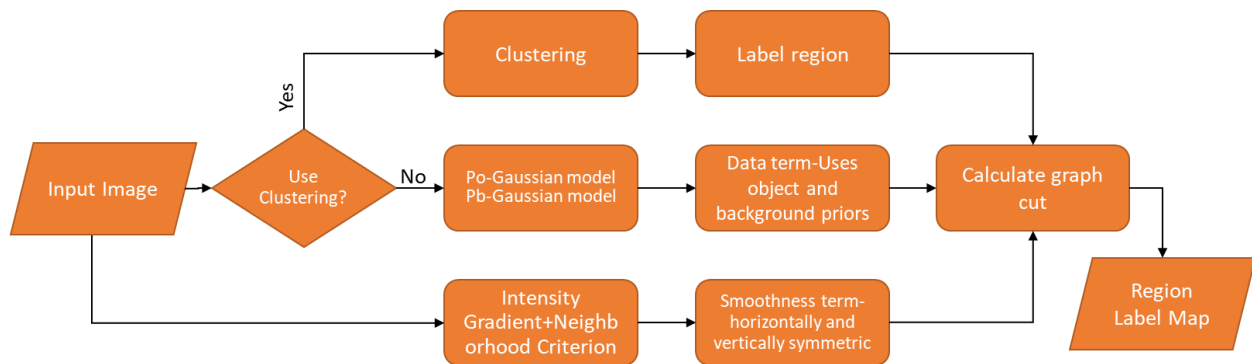


Figure 6: Flowchart of the Graph Cut method.

### How do we use graph cuts?

- Obtain a high-resolution (original) image, of an object of interest disposed in background
- By an outside process (user) to label partially the image with some pixels as object after labeling, other pixels as background. This initial partial labeling is referred to as seeds
- Here to produce a fully labeled, high-resolution image the process run the **graph cuts** algorithm

### Graph Cut

- Delete required number of edges so that each pixel is connected to exactly one label node
- Cost of a cut: sum of deleted edge weights
- Finding min cost cut equivalent to finding global minimum of energy function

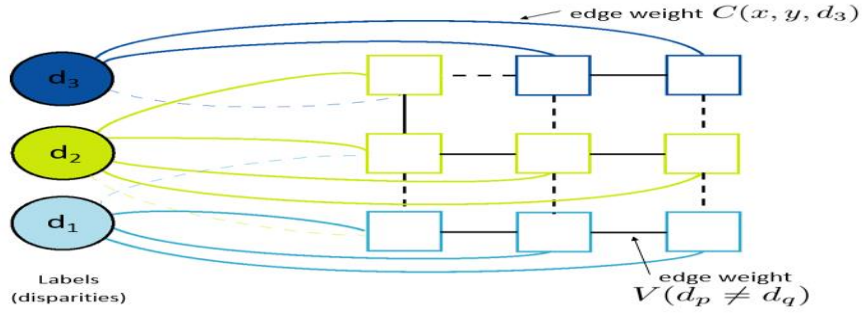


Figure 7: Energy minimization via graph cuts.[22]

## 2.10 Energy minimization using graph cut

In [22], to find a binary labeling that is globally optimal they describe the first use of Max-Flow/Min-Cut algorithms. Energy framework has been used for finding an estimate of the maximum a posteriori probability of a generalized Potts model Markov Random Field to find the binary labeling.

$$E(L) = \sum_{p \in P} D_p(L_p^i) + \lambda \sum_{p, q \in N} v_{p, q}(f_p, f_q)$$

Here in the above formula  $L$  is a labeling of the image  $P$ ,  $D_p$  is a data penalty function,  $V_{p, q}$  is an interaction potential and  $N$  is a neighborhood of pairs of neighboring pixels in the image  $P$ . The data penalty indicates a likelihood function and the interaction potentials force spatial coherence.

The partition of the set of vertices of a graph is a graph cut into two disjoint subsets and that is known as s-t cut or source-sink separation. To perform an s-t cut, to the graph vertices  $V$  in  $G = (V, E)$  are added two additional nodes, one is s - source node and other one is t - sink node. These represent the labels that can be assigned to pixels or voxels in image segmentation. The set of edges  $E$  of the constructed graph  $G_{st} = (V \cup s, t, E)$  is constructed by two types of edges, N-links



and T-links. N-links or neighboring links connect pairs of neighboring pixels [22] and T-links or terminal links connect the nodes in the graph to the terminal nodes  $s, t$ . All the graph edges have associated a cost: in the case of directed graphs, the cost of the edge  $(p, q)$  is different from the cost of the reverse edge  $(q, p)$ . The cost function to be minimized is defined as

$$E(f) = E_{data}(f) + E_{smooth}(f)$$

The min-cut of the weighted graph represents the segmentation that best separates the object from its background. Typical applications of graph cuts to image segmentation differ only in the definitions of  $D_p(L_p^i)$  and  $v_{p,q}(f_p, f_q)$ .

The data term costs correspond to the penalty associated to assigning the corresponding label to that pixel. Where  $E_{data}$  represents the costs and that is associated to the t-links. Data term is also known as regional term.

$$D(L_p^i) = -\log P(f_p | L_p^i)$$

Where  $i$  is a pixel,  $L_i$  is the label at  $i$ ,  $P(f_p | L_i^p)$  is the probability of the observed class (foreground/background).

The cost of a smoothness term represents the penalty for not assigning the two neighboring pixels to the same label.  $E_{smooth}$  represents the cost that is associated to the n-links.

It connects each pairwise combination of neighboring pixels  $(p, q)$  with a non-negative edge weight determined by a penalty for boundary discontinuity,  $V(p, q)$ . A frequent selection for the smoothness function is

$$V(p, q) = V(p, q) = \exp\left(-\frac{\|f_p - f_q\|^2}{2\sigma^2}\right) \frac{1}{\|p - q\|}$$

Where  $\sigma$  is a user-defined parameter and  $\|f_p - f_q\|$  is the Euclidean pixel distance for normalizing among edges of different length.

An s-t cut partitions the nodes into two subsets. The cost of a cut is equal to the cost of the edges in the cut and no path can be established between source and sink.

## CHAPTER III: GRAPH CUT SEGMENTATION WITH STATISTICAL PRIORS

Graph cut segmentation techniques detect objects or anatomical structures using prototypes of object classes corresponding to the terminal nodes. We first describe the unsupervised learning technique of K-means. Then we explain supervised learning using normal distribution models and Bayesian inference. Finally, we describe the applications of object detection in generic images and tissue identification in CT scans.

### 3.1 Learning Parametric Models for Tissues

We need to find  $P(f_p | L_p^i)$ ,  $i = 1, \dots, n$ , where  $n$  is the number of objects/classes. We estimate normal parametric distribution models from reference masks

$$P(f_p | L_p^i) = \frac{1}{\|2\pi\Sigma_i\|^{\frac{1}{2}}} \exp \left[ -\frac{1}{2} (f_p - M_i)^t \Sigma_i^{-1} (f_p - M_i) \right].$$

We may use unsupervised or supervised techniques to learn the parameters  $(M_i, \Sigma_i)$ .

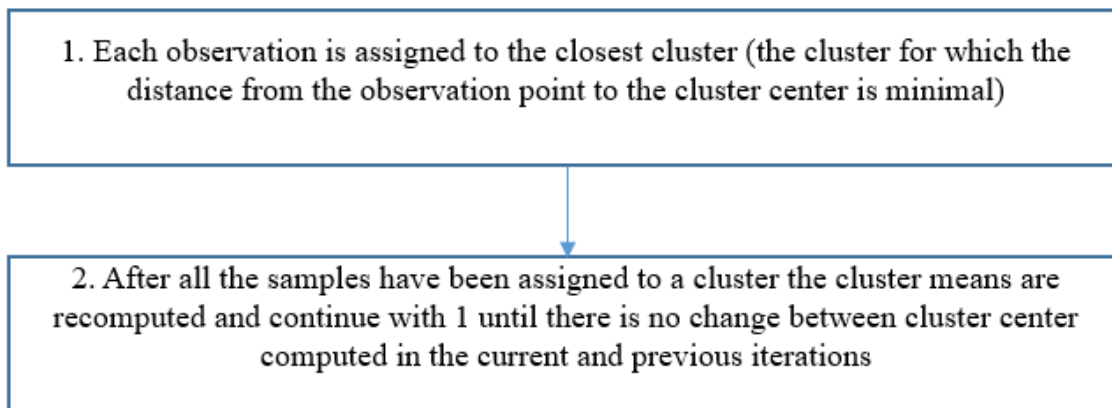
### 3.2 Unsupervised Learning: K-means clustering:

The K-means algorithm is one of the most popular algorithms used for clustering [18, 21]. It assumes that the data points are of the quantitative type and K-means algorithm can compute distances between points the data points. For a dataset of p-dimensional points, the most typical choice for inter-point distances is the squared Euclidean distance.

$$d(x_i, x'_i) = \sum_{j=1}^p (x_{ij}, x'_{ij})^2 \tag{3.1}$$

The center of each cluster is represented by the mean value of the points belonging to the cluster in all dimensions -  $\hat{x}_k = (\hat{x}_{1k}, \dots, \hat{x}_{pk})$ . The data points are associated to the cluster to which the average dissimilarity of the data point to the cluster center (cluster mean) is minimal. A description of the k-means algorithm is presented below:

Given that k (the number of clusters) is known, the algorithm begins by initializing the cluster means.



Sometimes the K-means algorithm is used for initializing the parameters in a distribution model type of clustering. We used K means algorithm for object detection to generic image and for tissue identification for medical image.

### 3.3 Segmentation using Supervised Learning for Prior Statistics

Another widely use of segmentation based on graph cut with Bayesian probability prior [23]. It is useful to have a more general concept of probability. It seems reasonable to apply the frequentist concept of probability to the random values of the observed variables  $t_n$ . However, we would like to address and quantify the uncertainty that surrounds the appropriate choice for the model

parameters  $w$ . We can use the machinery of probability theory to describe the uncertainty in model parameters such as  $w$ , or indeed in the choice of model itself. Using Bayesian probability prior, we can have better result than no prior method.

For generic images, we used statistics prior and for that, we draw a line in foreground and background of the image to partition images into object and background. Then we used it to the medical images to detect tissues. The maximum value of prior is 1 and minimum value is 0. We scale the images according to the prior. Here we will use Bayesian prior probability.

Bayes' theorem acquires a new significance [24]. In the boxes of fruit example, the observation of the identity of the fruit provided relevant information that altered the probability that the chosen box was the red one. In that example, Bayes' theorem converts a prior probability into a posterior probability by incorporating the evidence provided by the observed data. We can adopt a similar approach when making inferences about quantities such as the parameters  $w$  in the polynomial curve fitting example. We capture our assumptions about  $w$  before observing the data, in the form of a prior probability distribution  $p(w)$ . The effect of the observed data  $D = \{t_1, \dots, t_N\}$  is expressed through the conditional probability  $p(D|w)$ . Bayes' theorem, which takes the form

$$p(w|D) = \frac{p(D|w)p(w)}{p(D)} \quad 3.2$$

then allows us to evaluate the uncertainty in  $w$  after we have observed  $D$  in the form of the posterior probability  $p(w|D)$ . The quantity  $p(D|w)$  on the right-hand side of Bayes' theorem is evaluated for the observed data set  $D$  and can be viewed as a function of the parameter vector  $w$ , in which case it is called the likelihood function. It expresses how probable the observed data set is for different settings of the parameter vector  $w$ . Note that the likelihood is not a probability

distribution over  $w$ , and its integral with respect to  $w$  does not (necessarily) equal one. The denominator in (3.2) is the normalization constant, which ensures that the posterior distribution on the left-hand side is a valid probability density and integrates to one.

In the Bayesian paradigm, the likelihood function  $p(D \vee w)$  plays a central role. However, the manner in which it is used is fundamentally different in the Bayes theorem. From the Bayesian theorem there is only a single data set  $D$  (namely the one that is actually observed), and the uncertainty in the parameters is expressed through a probability distribution over  $w$ . One advantage of the Bayesian viewpoint is that the inclusion of prior knowledge arises naturally. Suppose, such as, that a fair-looking coin is tossed three times and lands heads each time. A classical maximum likelihood estimate of the probability of landing heads would give 1, implying that all future tosses will land heads! A Bayesian approach with any reasonable prior will lead to a much less extreme conclusion.

### **3.4 Object Detection and Recognition**

Nowadays images and video are ubiquitous. The field of vision research is all about machine learning and statistics. In order to "understand" a real-world scene, images and videos are detected and classified. Programming a computer and designing algorithms helps to understand what is in these images is the field of computer vision. Computer vision has many applications like image search, robot navigation, medical image analysis, photo management and many more. From a computer vision perspective, the image is a scene consisting of objects of interest and a background represented by everything else in the image. The relations and interactions among these objects are the key factors for scene understanding. In computer vision, object detection and recognition are two important tasks. The presence of an object and locations in the image determined by object

detection. Object recognition identifies the object class in the training database, to which the object belongs to. Object detection typically precedes object recognition. It can be preserved as a two-class object recognition, where one class represents the object class and another class represents non-object class [25]. Object detection can be divided into two types of detection-soft detection, which only detects the presence of an object, and hard detection, which detects both the presence and location of the object. Object detection field is typically carried out by searching each part of an image to localize parts, whose photometric or geometric properties match those of the target object in the training database. This can be accomplished by scanning an object template across an image at different locations, scales, and rotations, and a detection is declared if the similarity between the template and the image is sufficiently high. Their correlation measures the similarity between a template and an image region. It is noticed that image based object detectors are sensitive to the training data last several years.

Here we use graph cuts with object and background prototypes to detect and delineate an object. The use of terminal nodes is an advantage of graph cuts for detection algorithms. We will first use samples for each class that were determined by polylines that can be drawn over the object and background.

### **3.5 Automated Medical Image Segmentation Techniques**

Now a days Computed topography (CT) imaging are increasing for diagnosis, treatment planning and clinical studies so it has been almost compulsory to use computers to assist radiological experts in clinical diagnosis, treatment planning [25]. Reliable algorithms are required for the delineation of anatomical structures and other regions of interest (ROI). There are goals of computer-aided diagnosis are:

- i. If the process is automated there is a chance to have large number of cases with the same accuracy i.e. the results are not affected because of fatigue, data overload or missing manual steps.
- ii. Automated process can give fast and accurate results. High-speed computers are, now, available at modest costs, speeding up computer-based processing in the medical field.
- iii. Patient care can be extended to remote areas using information technology.

There is no universal algorithm for segmentation of every medical image. Each imaging system has its own specific limitations.

### **3.6 Computed Tomography Imaging.**

CT scan uses X-rays to obtain structural and functional information about the human body and it is an imaging modality. The CT image is reconstructed on the basis of X-ray absorption profile and is the reconstructed image. X-rays are electromagnetic waves and it is used in diagnosis based on its property that all matters and tissues differ in their ability to absorb X-rays.[26] Dense tissues such as the bones appear white on a CT film while soft tissues such as the brain or liver appear gray. The cavities filled with air such as lungs appear black. CT performs better in cases of trauma and emergent situations. It has high sensitivity for acute hemorrhage and provides better bone detail. CT is an important tool in medical imaging to supplement X-rays, medical ultrasonography (USG) and MR imaging. Although it is still expensive, it is the high standard in the diagnosis of a large number of different disease entities. It is more recently being used in early screening of diseases, for example CT colonography for patients with a high risk of colon cancer. CT scans are particularly used in medical imaging and the diagnosis of following body parts: brain, liver, chest, abdomen, thigh and pelvis, spine and for CT based angiography.



In case of thigh CT imaging, CT is the most commonly used imaging technique to detect the abnormality in subcutaneous adipose tissue (SAT), intermuscular fat, muscle, cortical bone and trabecular bone. There are relative advantages and disadvantages of CT. In general, CT is less costly than MR, more readily available, and most radiologists and many referring physicians have a relatively high degree of confidence in looking at CT images. Some studies, however, have found that CT is less sensitive and specific than MR for detection and characterization of focal hepatic disease.

### **3.7 Calculation of Priors for Segmentation of Medical Images**

Segmentation is the process partitioning of an image into regions with similar properties such as gray level, color, texture, brightness, and contrast. [28–26]. The role of segmentation is to divide the objects in an image into many parts; in case of medical image segmentation, the purpose is to study anatomical structure, identify Region of Interest (ROI) and measure volumetric, shape and density characteristics of anatomical structures.

Automatic segmentation of medical images is a complicated task because medical images are complex in nature and rarely have any simple linear feature. The output of segmentation algorithm is affected for partial volume effect, intensity inhomogeneity, presence of artifacts, and closeness in gray level of different soft tissue.

Many algorithms have been proposed in the field of medical image segmentation, medical image segmentation is a challenging problem. Different researchers have done the classification of segmentation techniques in different way. [26-38] Nowadays, from the medical image processing point of view, we have done the classification of segmentation techniques on the basis of gray level based and textural feature based techniques.

## CHAPTER IV: EXPERIMENTS, COMPARISONS AND RESULTS

### 4.1 Experiment 1: Object detection

We segmented 30 images from the GrabCut database using two different graph cut techniques GC with object priors and auto-conventional graph cuts. We show examples of segmentation using both methods in figure 8 (book and stone2). To segment the image we use statistical priors and draw polyline on images to provide samples for learning the class prototypes. Then, we compared the original image from the database to the segmented images.

After segmentation, we obtain two regions of the images, object and background. To compute segmentation accuracy we use Dice similarity coefficient (DSC) (Tables 1, 2 and 3 and Figure 9). This helped to determine the accuracy of the segmentation. All of these methods segment the images into two regions foreground and background. For every image in the GrabCut database, there is a reference segmentation map that corresponds to the original image.

The results in Tables 1, 2 and 3 show that the introduction of user-guided statistical priors for the object and the background improves segmentation accuracy by about 33%. This is a substantial accuracy increase that reduces the false detections for foreground and background.

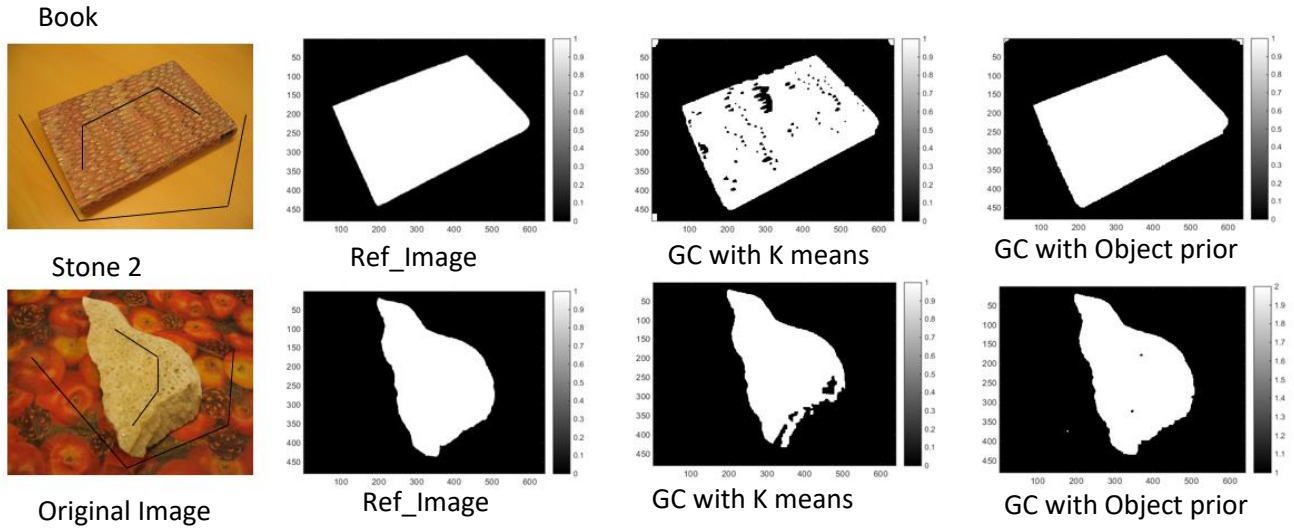


Figure 8: Segmentation results on two test images from our database. First column: original images, second column: reference images, third column: Auto (k-clustering) method, Fourth column: using object prior.

Table 1: Mean and Standard Deviation of two different graph cut techniques.

Graph cut method	DSC Mean %	DSC Standard Deviation %
GC with object prior	89.85	8.95
Auto- conventional graph cuts	56.87	30.36

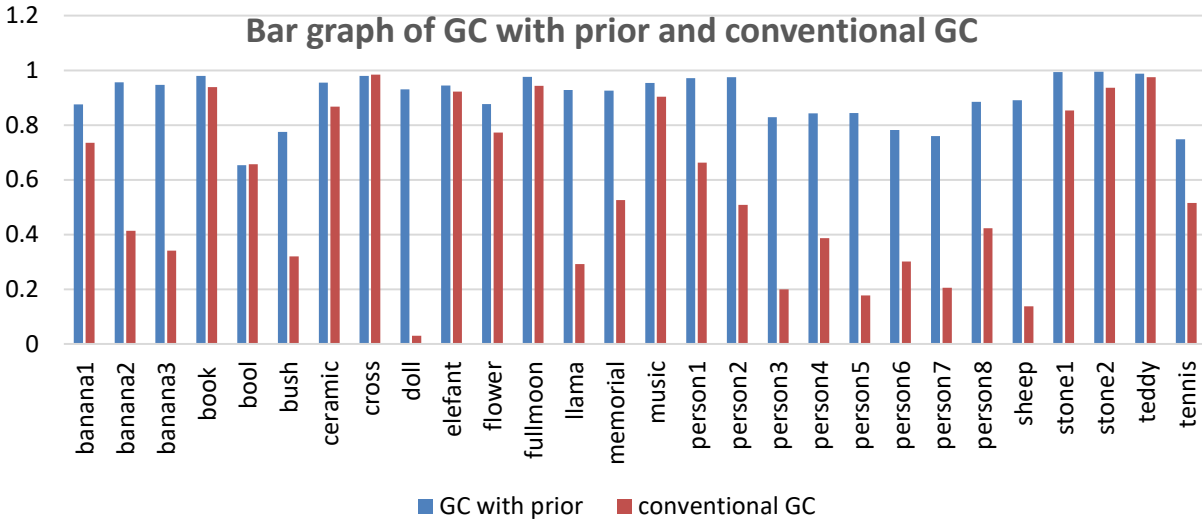


Figure 9: Graph corresponds to the two methods of Table 1,

Table 2: Result after using manual method – GC with object priors

banana1	0.8758	elephant	0.9447	person4	0.8428	tennis	0.7483
banana2	0.9557	flower	0.8769	person5	0.8437		
banana3	0.9472	Full moon	0.9758	person6	0.7818		
book	0.9793	llama	0.9284	person7	0.7601		
bool	0.6529	memorial	0.9257	person8	0.8849		
bush	0.775	music	0.9536	sheep	0.8904		
ceramic	0.955	person1	0.9711	stone1	0.9934		
cross	0.9798	person2	0.9751	stone2	0.9944		
doll	0.9307	person3	0.8291	teddy	0.9873		

Table 3: Results of Auto method- conventional graph cuts.

banana1	0.7346	elephant	0.9221	person4	0.3861	tennis	0.5149
banana2	0.414	flower	0.772	person5	0.1778		
banana3	0.3404	Full moon	0.9436	person6	0.3012		
book	0.9382	llama	0.2924	person7	0.2049		
bool	0.6563	memorial	0.5255	person8	0.4231		
bush	0.3202	music	0.903	sheep	0.1375		
ceramic	0.8668	person1	0.6627	stone1	0.853		
cross	0.9839	person2	0.5087	stone2	0.936		
doll	0.0293	person3	0.1992	teddy	0.9749		

#### 4.2 Experiment 2: Thigh CT tissue identification

We segmented 66 Thigh CT scans from the BLSA database using two different graph cut techniques GC with ROI priors and auto-conventional graph cuts with K means priors. All of the CT scans of this datasets were segmented by both methods. Then, we compared the original image from the database to the segmented images using the Dice Similarity Coefficient. After segmentation, we obtained four tissues from the images. All of these methods segment and identify the images into four tissues that is subcutaneous adipose tissue (SAT), cortical bone, muscle and trabecular bone. For every image in the Thigh BLSA CT images database there is a "perfect" segmented image that corresponds to the original image. The air, SAT, muscle, cortical bone were segmented into different regions represented by different colors on the color map. Based on the

examples and results of this experiment, the Graph Cut technique using statistical priors of CT intensities was achieved high accuracy rates – typically more than 90% - in distinguishing the different components of the lower leg. The K-means prior calculation was mostly affected by vast inequalities of tissue region cardinalities combined with tissue intensity distributions that were statistically difficult to identify. The performance of GC with K-means priors is improved by adding a step of tissue identification using max likelihood rule after completion of clustering.

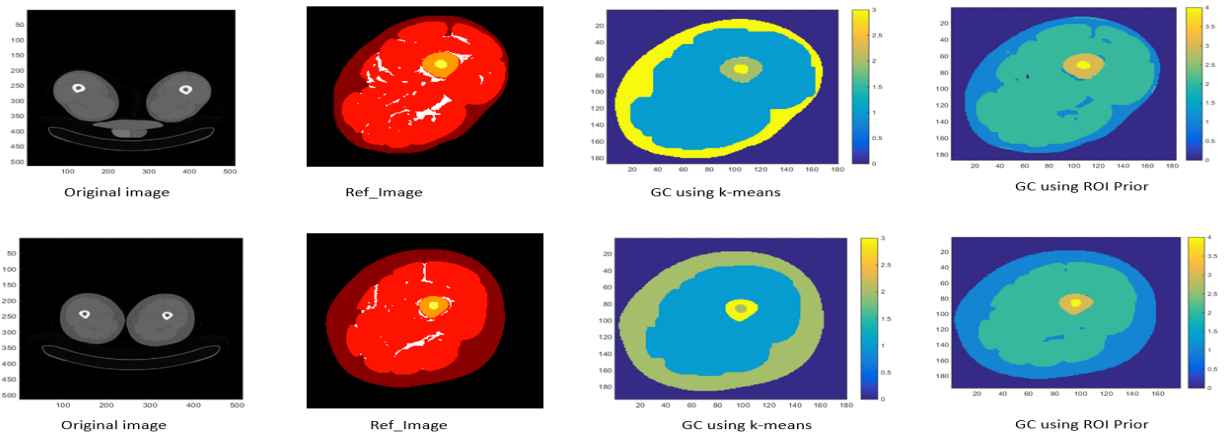


Figure 10: Tissue identification results on two test images from our Thigh BLSA CT images database. First column: original images, second column: reference images, third Column: GC with ROI prior, Fourth column: GC with K means prior.

Table 4: Mean and standard deviation of DSC for two graph cut techniques for each tissue of thigh CT

	Name of the tissues	DSC Mean %	DSC Standard Deviation %
Unsupervised GC with K-means priors without supervised centroid initialization	SAT	50.41	41.80
	Muscle	68.81	35.68
	Cortical bone	88.12	20.52
	Trabecular bone	88.17	20.15
	Over all tissues	73.88	29.54
	Unsupervised GC using calculated K-means priors with supervised centroid initialization	SAT	84.81
Muscle		93.87	2.88
Cortical bone		93.42	6.62
Trabecular bone		94.30	2.83
Over all tissues		91.60	7.932771
Proposed GC with ROI priors	SAT	91.37	4.68
	Muscle	95.99	1.26
	Cortical bone	92.21	6.72
	Trabecular bone	93.64	3.06
	Over all tissues	93.30	3.93

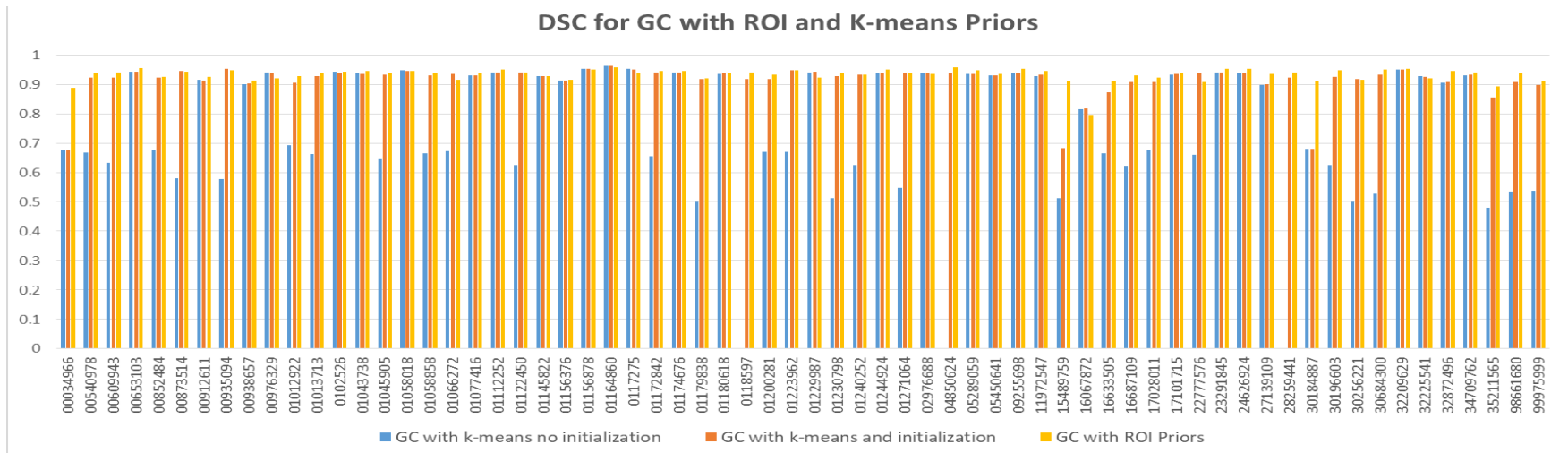
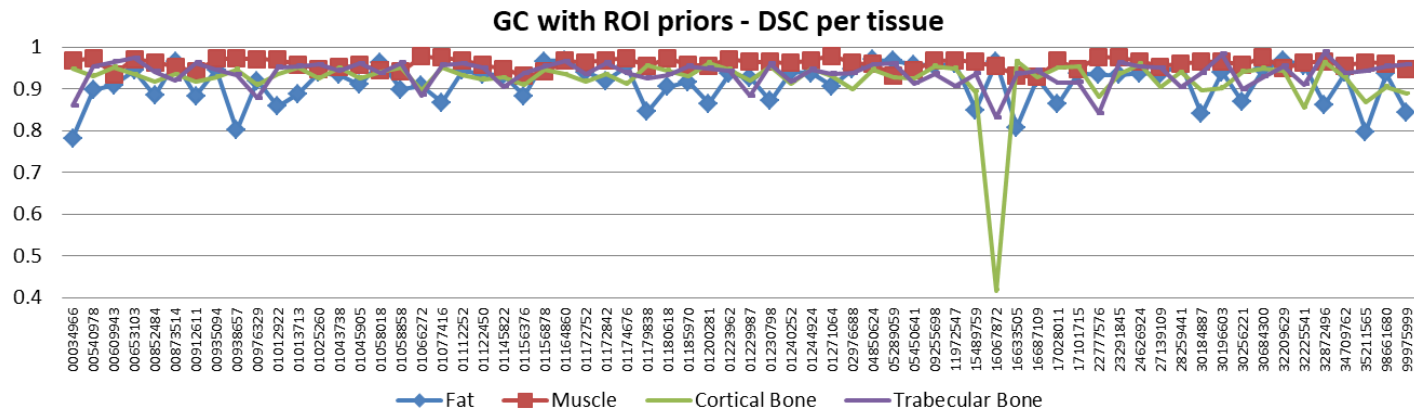


Figure 12: DSC bar graph when using graph cuts with the proposed supervised ROI priors and comparison with K means.



## CHAPTER V: CONCLUSION AND FUTURE WORK

### 5.1 Conclusion

In this thesis, we presented Graph Cuts methods using statistical priors for image segmentation and tissue identification. Image segmentation is the process of partitioning the image into the main objects of interest. We proposed methods for introducing supervised learning priors into the energy cost function. We evaluated the segmentation accuracy over 30 images from the computer vision GT database, and 66 mid-thigh CT scans. The method used for evaluating segmentation accuracy was the Dice Similarity Coefficient. Graph Cuts with supervised prior learning produced very good segmentation results for generic and medical images. This work can be extended in the following ways: develop different objective functions for optimization, apply graph cuts to region entities instead of pixels to improve segmentation accuracy, include region-based texture and color features in object and background prototypes, and segment different organs and anatomical structures in medical imaging data.

## References

1. O. Demetz, Graph Cuts in Computer Vision, pp. 3-13, M.Sc 2009.
2. Y. Boykov and M-P Jolly. Interactive graph cuts for optimal boundary and region segmentation of objects in n-d images. In ICCV, pp. 105–112, 2001.
3. N. Ahuja N. Xu and R. Bansal. Object segmentation using graph cuts based active contours. Computer Vision and Image Understanding, Volume 107, Issue 3, pp. 210–224, 2007.
4. A. M Sirghie .Abdominal fat segmentation using graph cut methods. Kongens Lyngby 2012 IMM-M.Sc.-2012-108.
5. J. Shi and J Malik. Normalized cuts and image segmentation. IEEE Transactions on Pattern Analysis and Machine Intelligence, Volume 22, Issue 8, pp. 888–905, 2000.
6. T. N. Janakiraman and P.V.S.S.R.C Mouli. Image segmentation based on minimal spanning tree and cycle. IEEE International Conference on Computational Intelligence and Multimedia Applications, pp 215–219, 2007.
7. T. Kanungo, An Efficient k-Means Clustering Algorithm: Analysis and Implementation, IEEE Transactions on Pattern Analysis and Machine Intelligence, Volume 24, Issue 7, pp. 881-890 JULY 2002.
8. S. K. brown. Experimental study on graph theoretic image analysis methods with applications to computer vision and biomedicine, M.Sc.- 2016.
9. F. C. Monteiro and A. Campilho, "Watershed framework to region-based image segmentation," in Proc. International Conference on Pattern Recognition, ICPR 19th, pp. 1-4, 2008.

10. M. Hameed, M. Sharif, M. Raza, S. W. Haider, and M. Iqbal, "Framework for the comparison of classifiers for medical image segmentation with transform and moment based features," *Research Journal of Recent Sciences*, vol. 2277, pp. 2502, 2012.
11. R. Patil and K. Jondhale, "Edge based technique to estimate number of clusters in k-means color image segmentation," in *Proc. 3rd IEEE International Conference on Computer Science and Information Technology (ICCSIT)*, pp. 117-121, 2010.
12. A. Fabijanska, "Variance filter for edge detection and edge-based image segmentation," in *Proc. International Conference on Perspective Technologies and Methods in MEMS Design (MEMSTECH)*, pp. 151-154, 2011.
13. F. Albregtsen, "Region and edge based segmentation", INF 4300 – Digital Image Analysis 21.09.2011.
14. M. Sezgin, B. Sankur, "Survey over image thresholding techniques and quantitative performance evaluation", Volume 13, Issue 1, pp. 146–165-2004.
15. O. J. Tobias, "Image segmentation by histogram thresholding using fuzzy sets", Vol. 11, Issue 12, DECEMBER 2002.
16. T. Garg, A Malik, "Survey on Various Enhanced K-Means Algorithms", *International Journal of Advanced Research in Computer and Communication Engineering* Vol. 3, Issue 11, November 2014.
17. K. Chitra , Dr. D.Maheswari, A Comparative Study of Various Clustering Algorithms in Data Mining, Vol. 6, Issue. 8, pp. 109 – 115, August 2017.
18. M.Vijayalakshmi, M.Renuka, "A Survey of Different Issue of Different clustering Algorithms Used in Large Data sets", *International Journal of Advanced Research in Computer Science and Software Engineering*, Volume 2, Issue 3, March 2012.

19. P. F. Felzenszwalb , Efficient Graph-Based Image Segmentation, Volume 59, Issue 2, pp. 167-181, September 2004.
20. T. H. Cormen, Clifford Stein, Ronald L. Rivest, and Charles E. Leiserson. Introduction to Algorithms. MIT Press, 2001.
21. O. Dank and P. Matula. Graph cuts and approximation of the euclidean metric on anisotropic grids. In VISAPP International Conference on Computer Vision Theory and Applications, pp. 68–73, Portugal, 2010. Institute for Systems and Technologies of Information, Control and Communication. Udleno ocenn Best Student Paper Award.
22. Y. Boykov, O. Veksler, and R. Zabih. Fast approximate energy minimization via graph cuts. IEEE Trans. Pattern Anal. Mach. Intell., Volume 23, Issue 11, pp. 1222– 1239, November 2001.
23. C. M. Bishop. Pattern Recognition and Machine Learning (Information Science and Statistics). Springer-Verlag New York, Inc., Secaucus, NJ, USA, 2006.
24. F. Jalled , Object Detection Using Image Processing, 23 Nov 2016.
25. N. Sharma and L M. Aggarwal. Automated medical image segmentation techniques. Volume 35, Issue 1 pp. 3-142010.
26. J.L. Prince, JM Links. Medical imaging signals and systems. Pearson Education. ISBN 0-13-065353-5, 2006.
27. R.C. Gonzalez, RE Woods. Digital image processing. 2nd ed. 2004. Pearson Education.
28. K.W. Pratt. Digital image processing. 3rd ed. Willey; 2001. pp. 551–87.
29. N.R. Pal, SH Pal. A review on image segmentation techniques. Pattern Recog. Volume 26, Issue 9, pp. 1277–94, 1993.

30. D.J. Withey, ZJ Koles. Three generations of medical image segmentation: Methods and available software. *Int J Bioelectromag*, Volume 9, Issue 2, pp. 67-68, 2007.
31. A. Macovski, *Medical imaging systems*. Volume 153, Issue 2, pp. 256 Prentice-Hall; 1983.
32. R. Popilock, K Sandrasagaren, Harris L, Kaser KA. CT artifact recognition for the nuclear technologist. *J Nucl Med Technol*. Volume 36, Issue 2, pp. 79–81, 2008
33. H. Li, R Deklerck, Cuyper BD, Hermanus A, Nyssen E, Cornelis J. Object recognition in brain CT-scans: Knowledge based fusion of data from multiple feature extractors. *IEEE T Med Imaging*. Volume 14, Issue 2, pp. 212–29, 1995.
34. D.L. Pham, JL Prince, Dagher AP, Xu C. An automated technique for statistical characterization of brain tissues in magnetic resonance imaging. *Int J Patt Rec Art Intel*. Volume 11, Issue 8, pp. 189–211 ,1997.
35. J. Jensen and C. B. Anker. *Segmentation of Abdominal Adipose Tissue in MRI in a Clinical Study of Growth and Diet*. DTU Information k, 2011.
36. O. Veksler. Image segmentation by nested cuts. In *IEEE Conference on Computer Vision and Pattern Recognition*, pp. 339–344, 2000.
37. D. Greig, B. Porteous, and A. Seheult. Exact Maximum A Posteriori Estimation for Binary Images. *Royal Journal on Statistical Society*, Volume 51, Issue 2, pp. 271– 279, 1989.
38. K. Li, X. Wu, D. Z. Chen, and M. Sonka. Optimal surface segmentation in volumetric images—agraph-theoretic approach. *IEEE TRANS. PATTERN ANAL. MACHINE INTELL*, Volume 28, Issue 1, pp. 119–134, 2006.
39. B. R. Dandu A. Chopra. Image segmentation using active contour model. *International Journal of Computational Engineering Research / ISSN:2250-3005*, Issue 2, pp. 819–822, 2012.

40. I. Laszio I. Fekete B. Dezso, R. Giachetta. Experimental study on graph-based image segmentation methods in the classification of satellite images. *EARSel eProceedings*, Volume 11, Issue 1, pp. 12–24, 2012.
41. Y. Boykov and V. Kolmogorov. An experimental comparison of mincut/max-flow algorithms for energy minimization in vision. *IEEE Transactions on pattern analysis and machine intelligence*, Volume 26, Issue 9, pp. 359–374, 2001.
42. P.F. Felzenszwalb and D.P. Huttenlocher. Efficient graph-based image segmentation. *International Journal of Computer Vision*, Volume 59, Issue 2, pp. 167–181, 2004.
43. A. V. Goldberg and E. Robert. Tarjan. A new approach to the maximum flow problem. *J. ACM*, Volume 35, Issue 4, pp. 921–940, October 1988.
44. C. Rafael. Gonzalez and E. Richard. Woods. *Digital Image Processing (3rd Edition)*. Prentice-Hall, Inc., Upper Saddle River, NJ, USA, 2006.
45. P. Elias, A. Feinstein, and C. E. Shannon. Note on maximum flow through a network. In *IRE Transactions on Information Theory IT-2*, pp. 117–199, 1956.
46. L. R. Ford Jr and D. R. Fulkerson. Maximal flow through a network. *Canadian Journal of Mathematics*, Volume 8, Issue 3, pp. 399–404, June 1956.
47. N. Ahuja N. Xu and R. Bansal. Object segmentation using graph cuts based active contours. *Computer Vision and Image Understanding*, Volume 107, Issue 3, pp. 210–224, 2007.
48. S. Makrogiannis G. Economou and S. Fotopoulos. A region dissimilarity relation that combines feature-space and spatial information for color image segmentation. *Systems, Man, and Cybernetics, Part B: Cybernetics, IEEE Transactions on*, Volume 35, Issue 1, pp. 44–53, 2005.

49. S. Makrogiannis, K. W. Fishbein C. Schreiber L Ferrucci S. Serai and R.G Spencer. Automated quantification of muscle and fat in the thigh from water,fat-, and nonsuppressed mr images. *Journal of Magnetic Resonance Imaging*, Volume 35, Issue 5, pp. 1152–1161, 2012.
50. S. Makrogiannis, G. Economou S. Fotopoulos, and N.G. Bourbakis. Segmentation of color images using multiscale clustering and graph theoretic region synthesis. *Systems, Man and Cybernetics, Part A: Systems and Humans*, *IEEE Transactions on*, Volume 35, Issue 2, pp. 224–238, 2005.
51. M Sonka, V Hlavac, and R Boyle. *Image Processing, Analysis, and Machine Vision*. Thomson-Engineering, 2007.
52. G Stockman and Linda G. Shapiro. *Computer Vision*. Prentice Hall PTR, Upper Saddle River, NJ, USA, 1st edition, 2001.
53. M H Fishbein, C Mogren, T Gleason, WR Stevens. Relationship of hepatic steatosis to adipose tissue distribution in pediatric nonalcoholic fatty liver disease. *J Pediatr Gastroenterol Nutr*, Volume 42, Issue 1, pp. 83–88, 2006 .
54. Fritz Albregtsen ,Region and edge based segmentation, INF 4300 – Digital Image Analysis 21.09.2011.
55. Ali Kemal Sinop Leo Grady, Banded graph cut segmentation algorithms with laplacian pyramids, Volume 2, LNCS 4191, pp. 896–903, 2006.